Supporting Information

Ultracompact Photonic Coupling Splitters Twisted by PTT Nanowires

Xiaobo Xing, Heng Zhu, Yuqing Wang, and Baojun Li*

State Key Laboratory of Optoelectronic Materials and Technologies, School of Physics and Engineering, Sun Yat-Sen University, Guangzhou 510275, China

* Corresponding author, e-mail: stslbj@mail.sysu.edu.cn

As a promising polymer, poly(trimethylene terephthalate) (PTT) possesses much small crystal modulus of 2.59 GPa, strong flexibility and larger than 90% elastic recovery, together with chemical stability and stain resistance.[1–5] In Figure S1, we show that the transmittance of the PTT film (25-μm amorphous film) is about 90% in the wavelength region of 400 to 2000 nm. Its good transparency from visible to near-infrared together with its relatively large refractive index (1.638)[6] can provide fine optical confinement for advanced nanowires and nanophotonic devices. PTT nanofibrous mats with diameters of 200–600 nm have been fabricated by electrospinning,[7] whereas the obtained nanowires by electrospinning with large surface roughness and length inhomogeneity would induce large optical loss. Using one-step direct drawing technique, we have fabricated flexible and elastic enough PTT nanowires (PNWs) exhibiting high surface smoothness and length uniformity. We further assembled ultracompact photonic coupling splitters with multiple input/output ports by twisting the PNWs.

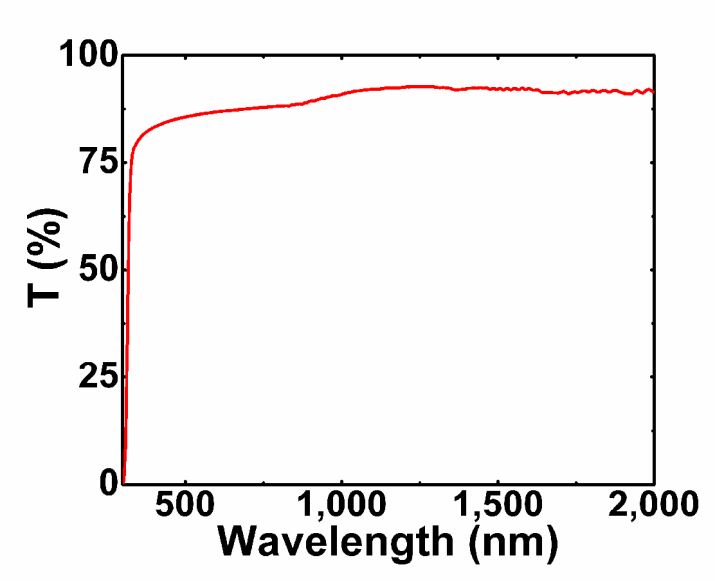

Figure S1. Room-temperature transmission spectrum of a 25-μm-thick amorphous PTT film. It shows the transmittance of about 90% in the wavelength region of 400 to 2000 nm.

Using one-step drawing process, we have obtained PNWs with diameters down to 60 nm. For comparison, a scanning electron microscope (SEM) image (Figure S2a) shows that a 167-nm-diameter PNW with length of about 155 μm is positioned together with a 1.26-μm-diameter straight PTT rod. Figure S2b shows that four 110-nm-diameter PNWs are bent and positioned together. Figure S2c demonstrates flexible and elastic connection by pulling the PNWs with diameters of 140 and 170 nm. To examine surface roughness of the PNWs, high-magnification transmission electron microscope (TEM) was done. Figure S2d shows a TEM image of a 190-nm-diameter nanowire, indicating no visible defect and irregularity on the surface of the PNWs. Typical average sidewall root-mean-square roughness of the PNW is 0.28 nm. The electron diffraction pattern (inset of Figure S2d) demonstrates that the obtained PNW is amorphous. The results demonstrate that the obtained PNWs exhibit high surface smoothness, length uniformity, high mechanical properties, and excellent flexibility.

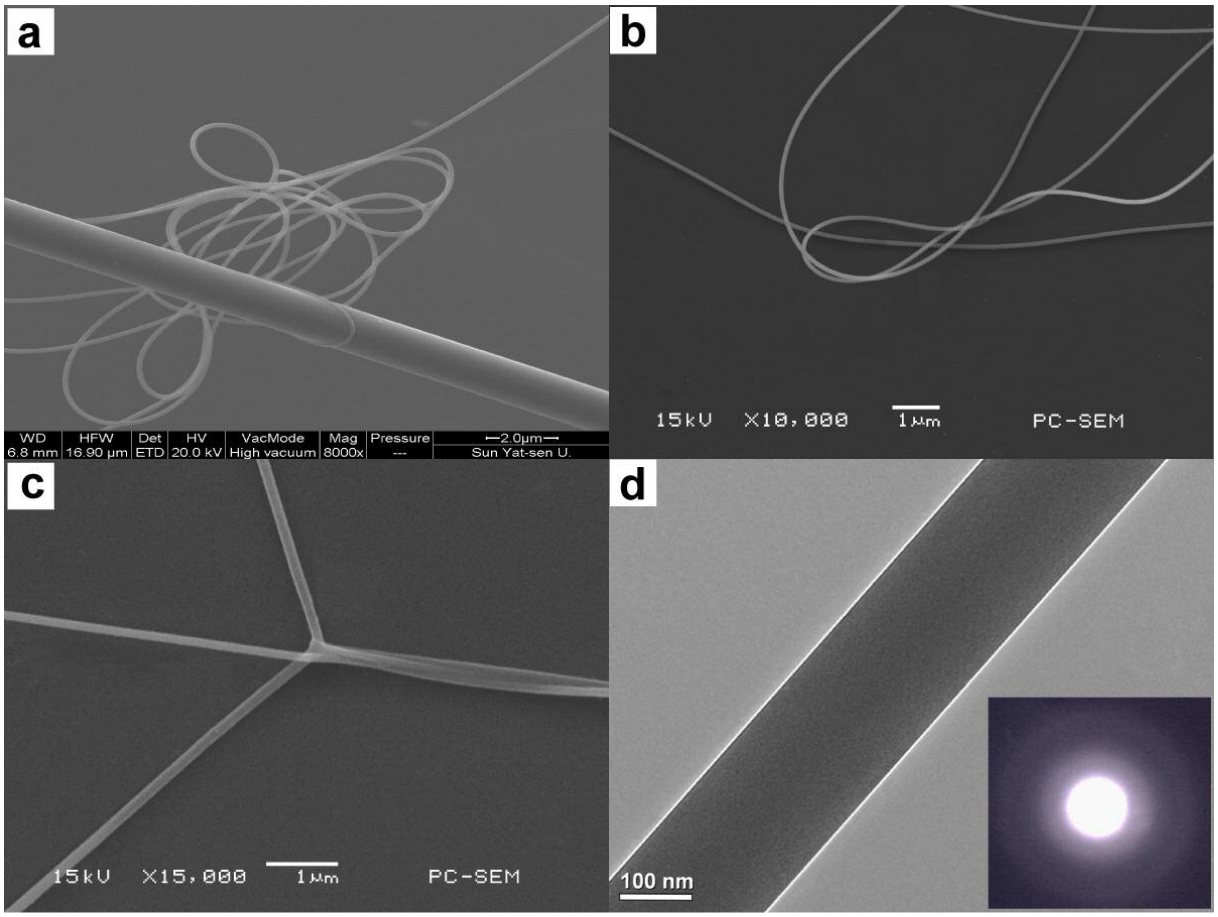

Figure S2. Electron micrographs of PTT nanowires and nanowire structures. a–c, SEM images: (a) Comparison of a 167-nm-diameter PNW (about 155 µm long) with a 1.26-µm-diameter straight PTT rod. (b) Four 110-nm-diameter PNWs are positioned together. (c) Flexible and elastic enough PNWs connection with diameters of 140 and 170 nm. (d) TEM image of a 190-nm-diameter PNW. The inset shows its electron diffraction pattern.

To investigate the coupling properties between the silica nanotaper (obtained by flame-heated technique)[8] and the PNW, we fixed the PNW by two microstage supports, and launched different wavelength lights from the silica nanotaper into the PNW by evanescent coupling.[9] As an example, we launched a 650 nm red light from a 520-nm-diameter silica nanotaper into a 400-nm-diameter PNW (Figure S3). We positioned the silica nanotaper and the PNW to form different crossing angles and adjusted them to reach maximum output power at the end of the PNW. Figure S3a shows that a red light from the silica nanotaper along the horizontal wire, no light was coupled into the vertical PNW except two visible scattering spots at the intersection and the end of the silica nanotaper. When the crossing

angle was changed to be 79° between the silica nanotaper and the PNW, abut 0.7% optical power was coupled into the PNW (Figure S3b). In this case, similar scattering spots were observed at the intersection and the end of the silica nanotaper. We found that the scattering spot at the intersection become very small when the crossing angle was changed to be 55° (Figure S3c), and the measured coupling efficiency is about 6.3%. Figures S3d and S3e further show optical images of crossing angles of 27° and 10°, while the measured coupling efficiencies are 14.5% and 36.1%, respectively. As shown in Figure S3a–e, strong scatterings at the end of the silica nanotaper are observed. At last, we positioned the silica nanotaper to be parallel with the PNW and adjusted the overlap length until reach maximum coupling efficiency. Figure S3f shows that most of the light is coupled into the PNW and the measured coupling efficiency is as high as 94.8%. Moreover, Figure S3g shows that the coupling efficiency increases with the decreasing of the crossing angle, because a smaller crossing angle induces a larger overlap area of optical field between the silica nanotaper and the PNW.

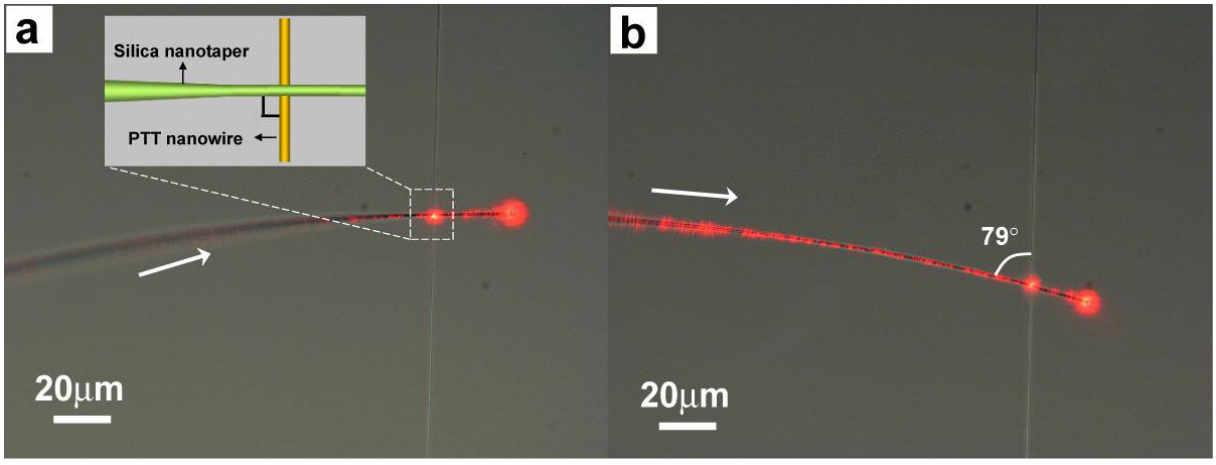

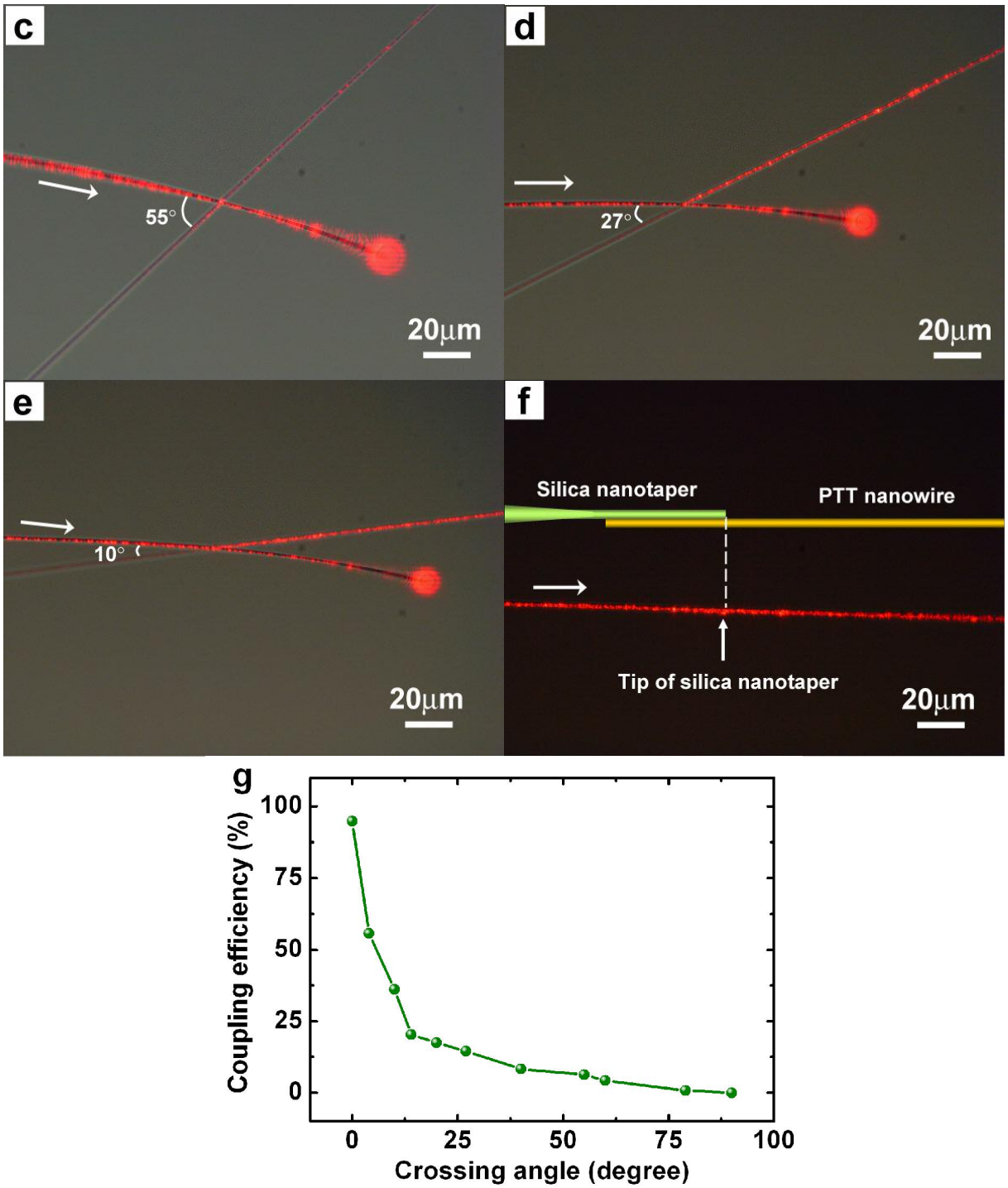

Figure S3. Evanescent coupling with different crossing angles. a–f, Optical microscope images of the evanescent coupling with different crossing angles of 90° (a), 79° (b), 55° (c), 27° (d), 10° (e), and 0° (f) between a 520-nm-diameter silica nanotaper and a 400-nm-diameter PNW. The white arrows show the propagation directions of the launched lights. The insets in green and yellow colors in a and f show the respective schematic diagrams of the coupling. (g) The coupling efficiency versus crossing angle.

Using the facile twisting technique, we fabricated $M\times N$ photonic coupling splitters. As examples, in

the following, we demonstrate 2×4, 3×3, and 5×5 photonic coupling splitters. Figure S4 shows that visible lights are coupled into a 2×4 coupling splitter with diameters of 330, 330, 330 and 320 nm for the right branches 1 to 4. The length of the twisted section is about 30 μm. The input branch B was formed by twisting three 330-, 330-, and 320-nm-diameter PNWs. Figure S4a shows that the red light is coupled into the branch A and split into four parts through the coupling region, with a splitting ratio of 26:26:26:22 for output branches 1 to 4. Figure S4b and 4c show that the green and blue lights launched from the branch B are divided into the branches 1 to 4 with splitting ratios of 30:21:20:29 and 26:25:25:24, respectively. The excess losses of the guided red, green, and blue lights are 0.674 to 0.779 dB, as shown in Figure S4d, where the sum of the input and output coupling losses is about 0.48 dB.

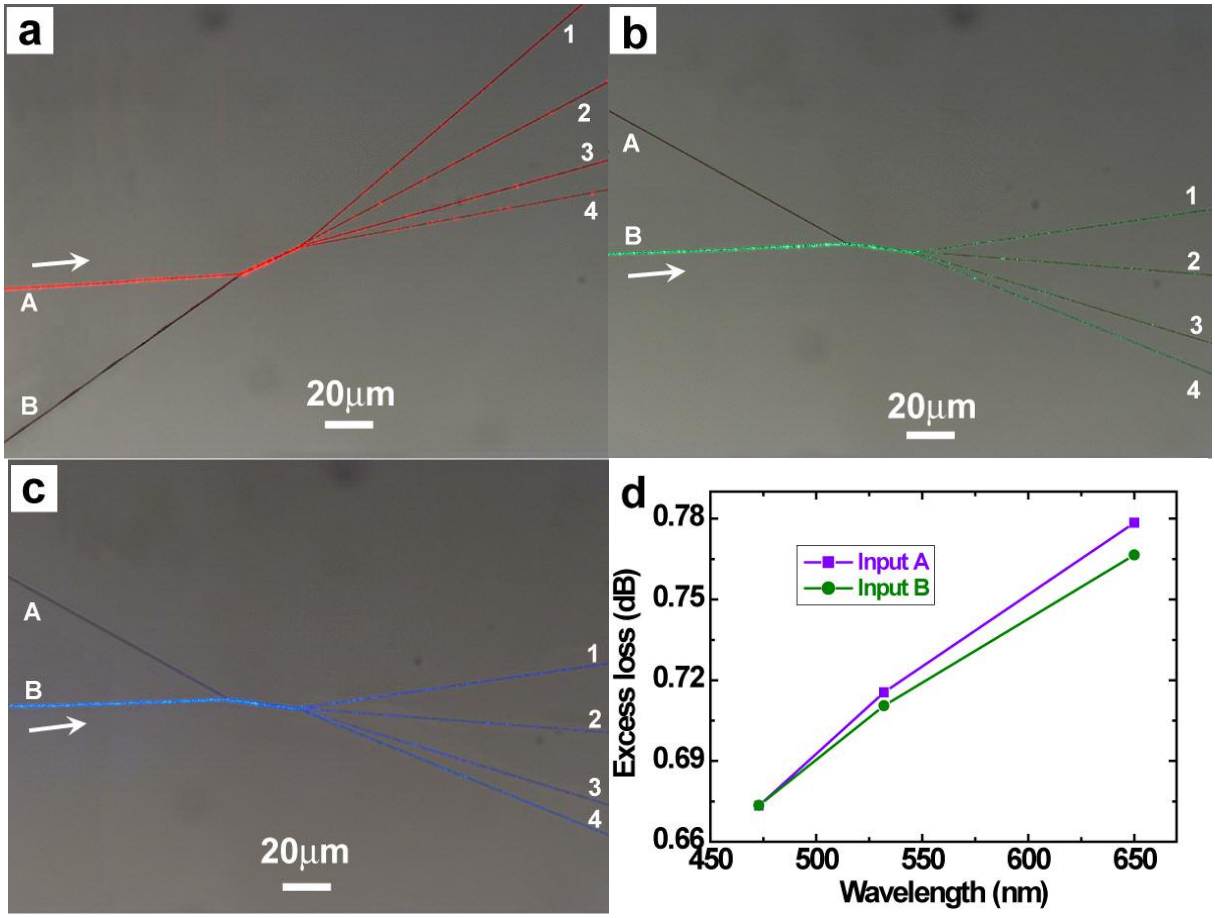

Figure S4. A 2×4 photonic coupling splitter. The diameters of the PNWs are 330, 330, 330 and 320 nm for right branches 1 to 4. Three PNWs with diameters of 330, 330, and 320 nm are twisted together to form the left input branch B. (a)–(c) Optical microscope images of the guided red, green, and blue lights, respectively. The arrows show the propagation directions of the launched lights. (d) Excess loss of the device for the guided red, green, and blue lights.

Figure S5 further shows a 3×3 coupling splitter cascaded by a 1×3 and a 2×3 coupling splitters, with diameters of 550, 530, and 480 nm for branches 1 to 3. The length of the coupling region of the 1×3 splitter is about 23 μm, and that of the 2×3 splitter is about 95 μm. The measured splitting ratios are 42:30:28 and 30:33:37 for output branches 1 to 3 when red (Figure S5a) and blue (Figure S5b) lights are launched into the branch A, respectively. The excess losses are 0.725 and 0.662 dB.

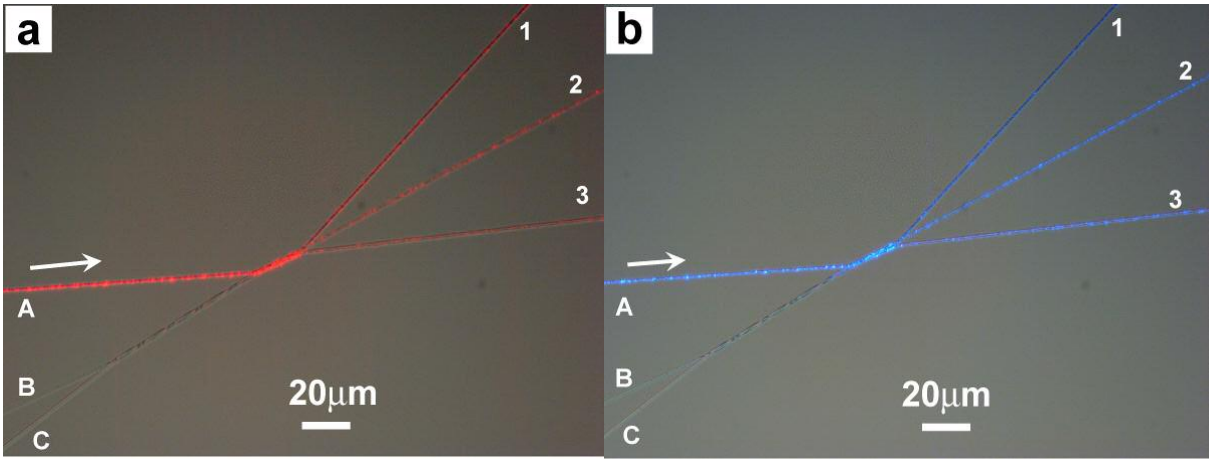

Figure S5. Optical microscope images of the guided red and blue lights in a 3×3 photonic coupling splitter cascaded by a 1×3 and a 2×3 coupling splitters. The diameters of the PNWs are 550, 530, and 480 nm for branches 1 to 3. The arrows show the propagation directions of the launched lights.

Figure S6a shows that red light is launched into the branch D of a 5×5 splitter, which was assembled by twisting five PNWs with diameters of 410, 450, 470, 470 and 470 nm for branches 1 to 5. The splitting ratio is 16:17:24:23:20 for the branches 1 to 5 and the excess loss is 0.775 dB. Figure S6b further shows a 5×5 coupling splitter with diameters of 480, 450, 350, 380 and 400 nm for branches 1 to 5. Green light is launched into the branch B and split into five parts with a splitting ratio of 55:20:10:9:6 and an excess loss of 0.765 dB. Figure S6c shows that blue lights are simultaneously launched into the branches A, B, and C of a 5×5 coupling splitter, which was assembled by twisting five PNWs with diameters of 420,

540, 410, 550 and 570 nm for branches 1 to 5. The measured splitting ratio is 15:23:16:25:21 for branches 1 to 5 and the excess loss is 0.68 dB.

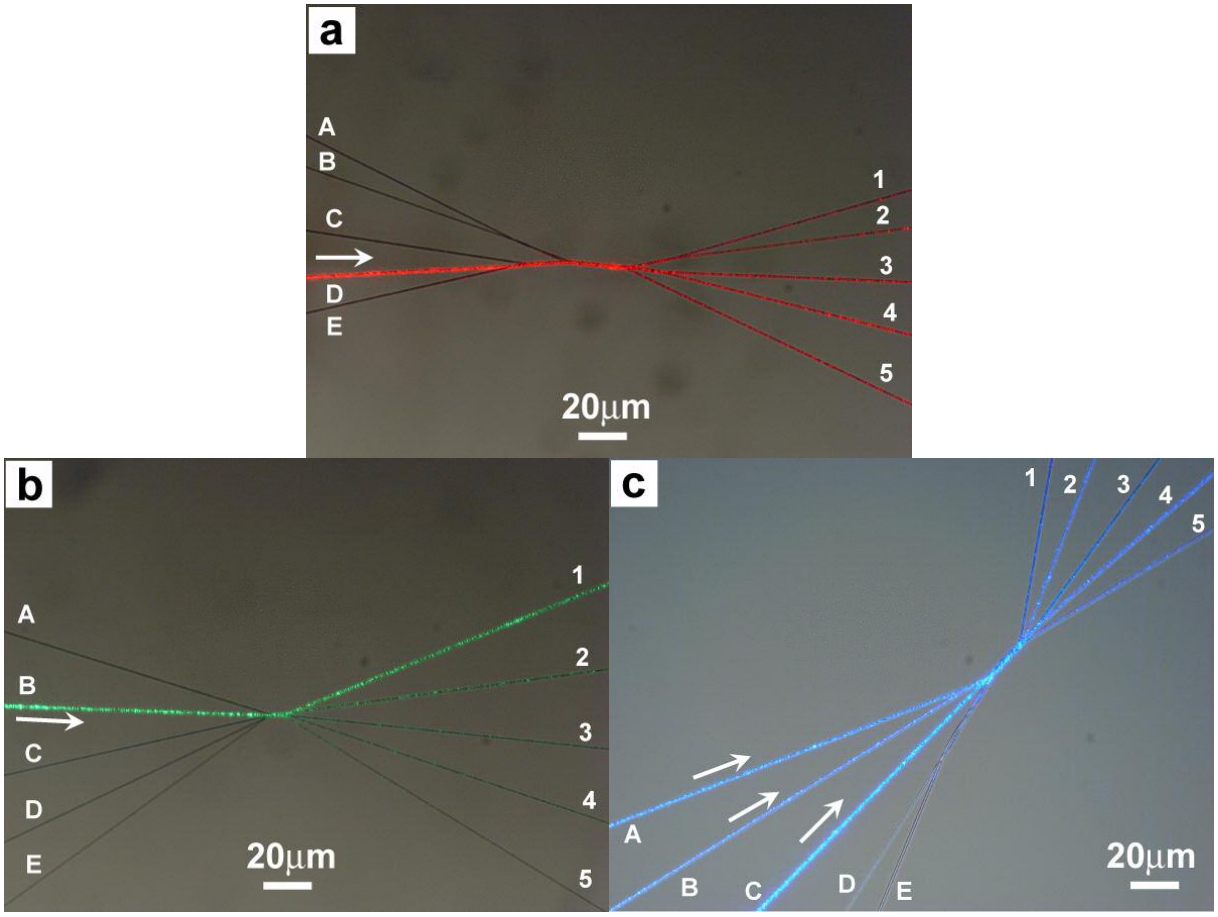

Figure S6. Optical microscope images of three 5×5 photonic coupling splitters. (a) Red light is launched into the branch D of a 5×5 splitter with diameters of 410, 450, 470, 470 and 470 nm from branches 1 to 5. (b) Green light is launched into the branch B of a 5×5 splitter with diameters of 480, 450, 350, 380 and 400 nm from branches 1 to 5. (c) Blue lights are simultaneously launched into the branches of A, B, and C of a 5×5 splitter with diameters of 420, 540, 410, 550 and 570 nm from branches 1 to 5. The arrows show the propagation directions of the launched lights.

Supporting References

(1) Lyoo, W. S.; Lee, H. S.; Ji, B. C.; Han, S. S.; Koo, K.; Kim, S. S.; Kim, J. H.; Lee, J.-S.; Son, T. W.; Yoon, W. S. *J. Appl. Polym. Sci.* **2001**, *81*, 3471.

(2) Chuah, H. H. *Macromolecules* **2001**, *34,* 6985.

(3) Kelsey, D. R.; Kiibler, K. S.; Tutunjian, P. N. *Polymer* **2005**, *46*, 8937.

(4) Hwo, C.; Forschner, T.; Lowtan, R.; Gwyn, D.; Cristea, B. *J. Plastic Film & Sheeting* **1999**, *15,* 219.

(5) Chuah, H. H.; Chang, B. T. A. *Polym. Bull.* **2001**, *46*, 307.

(6) Chuah, H. H. *J. Polym. Sci.*: *Part B*: *Polym. Phys.* **2002**, *40*, 1513.

(7) Khil, M. S.; Kim, H. Y.; Kim, M. S.; Park, S. Y.; Lee, D. R. *Polymer* **2004**, *45*, 295.

(8) Tong, L.; Gattass, R. R.; Ashcom, J. B.; He, S.; Lou, J.; Shen, M.; Maxwell, I.; Mazur, E. *Nature* **2003**, *426*, 816.

(9) Huang, K. J; Yang, S. Y.; Tong, L. M. *Appl. Opt.* **2007**, *46*, 1429.